Deformation of hypernuclei studied with antisymmetrized molecular dynamics

M. Isaka
Department of Cosmosciences, Graduate School of Science, Hokkaido University, Sapporo 001-0021, Japan

M. Kimura
Creative Research Institution (CRIS), Hokkaido University, Sapporo 060-0810, Japan

A. Dote
Institute of Particle and Nuclear Studies, KEK, Tsukuba, Ibaraki 305-0801, Japan

A. Ohnishi
Yukawa Institute for Theoretical Physics, Kyoto University, Kyoto 606-8502, Japan
(Received 1 December 2010; revised manuscript received 3 February 2011; published 27 April 2011)

An extended version of antisymmetrized molecular dynamics was developed to study the structure of *p*-*sd* shell hypernuclei. By using an effective ΛN interaction, we investigated the energy curves of ${}^{9}_{\Lambda}$Be, ${}^{13}_{\Lambda}$C, and ${}^{20,21}_{\Lambda}$Ne as a function of nuclear quadrupole deformation. The changes to nuclear deformation caused by Λ particles are discussed. We found that Λ in the *p* wave enhances nuclear deformation, while that in the *s* wave reduces it. This effect is most prominent in ${}^{13}_{\Lambda}$C. The possibility of parity inversion in ${}^{20}_{\Lambda}$Ne is also examined.

DOI: 10.1103/PhysRevC.83.044323 PACS number(s): 21.80.+a, 02.70.Ns, 27.20.+n, 27.30.+t

I. INTRODUCTION

One of the unique and interesting aspects of hypernuclei is the structure change caused by the hyperon as an impurity. Many theoretical works have suggested that such phenomena, caused by a Λ particle, result in changes of deformation [1–5], shrinkage of the intercluster distance [1,2], and creation of the supersymmetric (genuine) hypernuclear state [2,6–9]. Owing to experimental developments, some of these phenomena have been observed in light *p*-shell hypernuclei. As examples, we can refer to the reduction of B($E2$) in ${}^{7}_{\Lambda}$Li [10] and the identification of the supersymmetric (genuine) hypernuclear state in ${}^{9}_{\Lambda}$Be [11–13].

Today, we expect that a new experimental facility at the Japan Proton Accelerator Research Complex (J-PARC) will reveal spectral information about both the *p*-*sd* shell and neutron-rich hypernuclei. Since the normal forms of these nuclei have a variety of structures, such as a coexistence of shell and cluster structure [14–16] and novel exotic clustering [17–21], there must be many interesting phenomena peculiar to hypernuclei to be found. Indeed, several pioneering works have predicted exotic structures in *sd*-shell hypernuclei, such as parity inversion in ${}^{20}_{\Lambda}$Ne [7] and various rotational bands in ${}^{21}_{\Lambda}$Ne [22]. These works have been based on rather limited knowledge of the ΛN interaction. Since our knowledge of this interaction has been greatly increased by recent theoretical and experimental efforts [13,23–27], we are now able to perform a more quantitative and systematic study of the structure changes in Λ hypernuclei. Such a study will reveal the dynamics and many interesting aspects of the baryon many-body problem.

To perform such a systematic and quantitative study of *sd*-shell and neutron-rich Λ hypernuclei, we have developed an extended version of antisymmetrized molecular dynamics (AMD) [18,28–31], which we shall call HyperAMD. AMD has been successful at describing various exotic structures of neutron-rich nuclei and highly excited states of stable nuclei. Therefore, HyperAMD is suitable for describing the structure change and exotic structure of hypernuclei.

In this study, we introduce HyperAMD and focus on changes in nuclear quadrupole deformation caused by a Λ particle. By applying HyperAMD to ${}^{9}_{\Lambda}$Be, ${}^{13}_{\Lambda}$C, ${}^{20}_{\Lambda}$Ne, and ${}^{21}_{\Lambda}$Ne with a YNG-ND ΛN interaction [32], it is found that the Λ particle changes nuclear quadrupole deformation. While a Λ particle in the *s* wave reduces quadrupole deformation, as expected, one in the *p* orbital increases it. Among the calculated hypernuclei, ${}^{13}_{\Lambda}$C has shown the most drastic change of the nuclear deformation. We also find that the binding energy of a Λ particle depends on the structure of the core nucleus. Namely, the Λ in an *s* wave coupled to the deformed core nucleus has smaller binding than does one coupled to a spherical core. On the contrary, the Λ in a *p* wave coupled to the deformed core has greater binding than does one coupled to a spherical core. This contradicts the findings of a preceding study [7], in which the parity inversion of ${}^{20}_{\Lambda}$Ne was predicted.

This paper is organized as follows. In the next section, we explain the theoretical framework of HyperAMD. In Sec. III, the changes in energy curves as a function of quadrupole deformation are presented. The trends of these change and theirs origin are discussed. The final section summarizes this work.

II. THEORETICAL FRAMEWORK

In this section, we introduce the theoretical framework of HyperAMD. As compared to the coupled-channel AMD that describes the multistrangeness system [33], it has a better description of the hyperon single-particle wave function, but it does not treat multistrangeness and is limited to single-Λ hypernuclei.

A. Wave function

A single-Λ hypernucleus consists of A nucleons and a Λ particle and is described by the wave function that is the eigenstate of the parity:

$$\Psi^{\pm} = \hat{P}^{\pm}\Psi_{\rm int}, \tag{1}$$

where $\hat{P}^{\pm}$ is the parity projector, and the intrinsic wave function $\Psi_{\rm int}$ is given by the direct product of the single Λ particle wave function φ_Λ and the wave function of A nucleons Ψ_N,

$$\Psi_{\rm int} = \varphi_\Lambda \otimes \Psi_N. \tag{2}$$

The nuclear part is described by a Slater determinant of nucleon single-particle wave packets,

$$\Psi_N = \frac{1}{\sqrt{A!}} \det\{\psi_i(\boldsymbol{r}_j)\}, \tag{3}$$

$$\psi_i(\boldsymbol{r}_j) = \phi_i(\boldsymbol{r}_j)\cdot\chi_i\cdot\eta_i, \tag{4}$$

$$\phi_i(\boldsymbol{r}) = \prod_{\sigma=x,y,z}\left(\frac{2\nu_\sigma}{\pi}\right)^{1/4} \exp\left\{-\nu_\sigma(r-Z_i)_\sigma^2\right\}, \tag{5}$$

$$\chi_i = \alpha_i\chi_\uparrow + \beta_i\chi_\downarrow, \tag{6}$$

$$\eta_i = \text{proton or neutron}, \tag{7}$$

where ψ_i is the ith nucleon single-particle wave packet, consisting of spatial ϕ_i, spin χ_i, and isospin η_i parts. The spatial part ϕ_i is represented by a deformed Gaussian. Its centroid, $\boldsymbol{Z}_i$, is a complex-valued three-dimensional vector. The width parameters ν_σ are real numbers and take an independent value for each direction, but are common to all nucleons. The spin part is parametrized by the complex parameters α_i and β_i, and the isospin part is fixed to either a proton or neutron. $\boldsymbol{Z}_i$, ν_σ, α_i, and β_i are the variational parameters of the nuclear part.

To describe the various wave functions of the Λ particle, the Λ single-particle wave function is represented by the superposition of Gaussian wave packets,

$$\varphi_\Lambda(\boldsymbol{r}) = \sum_{m=1}^{M} c_m\varphi_m(\boldsymbol{r}), \quad \varphi_m(\boldsymbol{r}) = \phi_m(\boldsymbol{r})\cdot\chi_m, \tag{8}$$

$$\phi_m(\boldsymbol{r}) = \prod_{\sigma=x,y,z}\left(\frac{2\nu_\sigma\rho}{\pi}\right)^{1/4} \exp\left\{-\nu_\sigma\rho(r-z_m)_\sigma^2\right\}, \tag{9}$$

$$\chi_m = a_m\chi_\uparrow + b_m\chi_\downarrow, \tag{10}$$

$$\rho \equiv \frac{m_\Lambda}{m_N}. \tag{11}$$

Again, each wave packet is parametrized by the centroid of the Gaussian $\boldsymbol{z}_m$, the spin direction a_m, and b_m. $\boldsymbol{z}_m$, a_m, b_m, and c_m are the variational parameters of the Λ part. The width parameter ν_σ are equal to those of the nuclear part. The number of the superposition M is taken to be large enough to allow the energy convergence of the variational calculation.

B. Hamiltonian

The Hamiltonian used in this study is given as

$$\hat{H} = \hat{T}_N + \hat{V}_{NN} + \hat{V}_{\rm Coul} + \hat{T}_\Lambda + \hat{V}_{\Lambda N} - \hat{T}_g. \tag{12}$$

Here, $\hat{T}_N$, $\hat{T}_\Lambda$, and $\hat{T}_g$ are the kinetic energies of the nucleons, the kinetic energy of the Λ particle, and the center-of-mass motion. Since we have superposed Gaussian wave packets to describe the Λ single-particle wave function, it is rather time consuming to remove the spurious motion of the center of mass exactly. To reduce this spurious motion, we keep the center of mass of the wave packets at the origin of the coordinate,

$$\sum_{i=1}^{A}\boldsymbol{Z}_i + \sum_{m=1}^{M}\sqrt{\rho}\boldsymbol{z}_m = 0. \tag{13}$$

We expect that the spurious energy is not large in sd-shell hypernuclei, since the number of nucleons is much larger than the hyperon. A similar method has been applied in other AMD studies [28].

Our model wave function is designed to describe low-momentum phenomena, as in the case of the conventional shell model, and we shall use the low-momentum effective interaction. We have used the Gogny D1S interaction [34] as an effective nucleon-nucleon interaction $\hat{V}_{\rm NN}$, which has been successfully applied to stable and unstable normal nuclei. As an effective ΛN interaction, we have used the central part of the YNG-ND interaction [32]. The YNG-ND interaction depends on the nuclear Fermi momentum k_F through the density dependence of the $\boldsymbol{G}$ matrix in the nuclear medium. In this work, we apply $k_F = 1.14$ and $1.17\ \text{fm}^{-1}$, respectively, for ${}^{9}_{\Lambda}$Be and ${}^{13}_{\Lambda}$C, which are so determined as to approximately reproduce the binding energy of Λ in an s wave. For ${}^{20}_{\Lambda}$Ne and ${}^{21}_{\Lambda}$Ne, we apply the same value as for ${}^{13}_{\Lambda}$C, since there are no experimental data. The Coulomb interaction is approximated by the sum of seven Gaussians.

C. Frictional cooling method with constraints

Using the frictional cooling method, the variational parameters of the model wave function are so determined that the total energy is minimized under the constraints. We have imposed two constraints on the variational calculation. The first is on the nuclear quadrupole deformation parameter β that is calculated by adding the parabolic potential,

$$\langle\hat{V}_\beta\rangle = v_\beta(\beta-\beta_0)^2, \tag{14}$$

to the total energy. Here, β denotes the quadrupole deformation of the nuclear wave function Ψ_N [28]. The deformation of the nuclear part becomes equal to β_0 after the variation. It is noted that there are no constraints on the nuclear quadrupole deformation γ and the deformation of the Λ single-particle wave function. They have the optimum value after the variational calculation for each given value of β_0.

Another constraint is on the Λ single-particle wave function,

$$\hat{V}_s = \Lambda|\varphi_s\rangle\langle\varphi_s|, \tag{15}$$

$$\langle\boldsymbol{r}|\varphi_s\rangle = \exp\{-\rho\bar{\nu}r^2\}, \tag{16}$$

$$\bar{\nu} = \sqrt[3]{\nu_x\nu_y\nu_z}. \tag{17}$$

By using a sufficiently large value for Λ, this potential forbids Λ in an s wave. Therefore, by switching this potential on and

off, we obtain the hypernuclear states in which a Λ particle dominantly occupies the s and p waves, respectively.

The total energy plus constraint potentials,

$$E' = \frac{\langle\Psi^{\pm}|\hat{H}|\Psi^{\pm}\rangle}{\langle\Psi^{\pm}|\Psi^{\pm}\rangle} + \langle\hat{V}_s\rangle + \langle\hat{V}_\beta\rangle, \tag{18}$$

is minimized using the frictional cooling method. The imaginary time development equations of the variational parameters are given as,

$$\frac{dX}{dt} = \frac{\mu}{\hbar}\frac{\partial E'}{\partial X^*}, \underline{a} \tag{19}$$

$$X = \boldsymbol{Z}_i, z_m, \alpha_i, \beta_i, a_m, b_m, \nu_\sigma, \nu_i^\Lambda, \tag{20}$$

where μ is an arbitrary negative real number. It is easy to prove that E' decreases over time, and after sufficient time steps we obtain the energy minimum under the constraint. By this method, we obtain the hypernuclear wave function for a given β_0, the total parity and the Λ single-particle orbital. In the present work, Λ dominantly occupies an s or a p wave, and we shall use the notation Λ_s and Λ_p for them. Combined with the parity projection, we obtain four different configurations in which Λ_s and Λ_p couple to the positive- and negative-parity states of the core. These are denoted $\Psi_N^+ \otimes \Lambda_s$, $\Psi_N^- \otimes \Lambda_s$, $\Psi_N^+ \otimes \Lambda_p$, and $\Psi_N^- \otimes \Lambda_p$ in the following discussion.

III. RESULTS AND DISCUSSION

A. General trend of the energy curves

We have performed the variational calculation for ${}^{9}_{\Lambda}$Be, ${}^{13}_{\Lambda}$C, ${}^{20}_{\Lambda}$Ne, and ${}^{21}_{\Lambda}$Ne. To illustrate the changes in nuclear deformation, Fig. 1 shows the energy curves of hypernuclear states with different configurations and the corresponding normal nuclei as functions of deformation β. Each energy curve has an energy minimum shown by the open circle, and the binding energies, quadrupole deformation, and radius at the minimum are listed in Table I. The binding energy of Λ is

TABLE I. Calculated total and Λ binding energies B and B_Λ, in MeV, quadrupole deformation parameters β and γ, and the root-mean square radius in fm at the minimum of each energy curve. The central values of the observed energies [12,13,35,36] are also listed in parentheses. The energies for the Λ_p states of ${}^{9}_{\Lambda}$Be and ${}^{13}_{\Lambda}$C are estimated from the observed excitation energies given in Ref. [13].

		B	B_Λ	β	γ	$\sqrt{\langle r^2\rangle}$
^{8}Be	Ψ_N^+	51.2(56.5)	–	0.68	1.9	2.50
${}^{9}_{\Lambda}$Be	$\Psi_N^+ \otimes \Lambda_s$	56.9(63.2)	5.75(6.71)	0.65	1.9	2.44
	$\Psi_N^+ \otimes \Lambda_p$	50.4(56.7)	−0.77(0.19)	0.71	1.7	2.53
^{12}C	Ψ_N^+	87.7(92.2)	–	0.27	60.0	2.42
	Ψ_N^-	75.5(82.5)	–	0.45	45.4	2.56
${}^{13}_{\Lambda}$C	$\Psi_N^+ \otimes \Lambda_s$	99.3(103.9)	11.6(11.69)	0.00	–	2.32
	$\Psi_N^+ \otimes \Lambda_p$	88.2(93.8)	0.46(1.65)	0.30	55.1	2.42
	$\Psi_N^- \otimes \Lambda_s$	86.2	−1.5	0.40	42.5	2.49
^{19}Ne	Ψ_N^+	142.6(143.7)	–	0.27	0.6	2.81
	Ψ_N^-	137.9(143.5)	–	0.45	0.5	2.91
${}^{20}_{\Lambda}$Ne	$\Psi_N^+ \otimes \Lambda_s$	159.4	16.8	0.25	0.6	2.76
	$\Psi_N^+ \otimes \Lambda_p$	148.4	5.74	0.30	0.9	2.81
	$\Psi_N^- \otimes \Lambda_s$	154.0	11.4	0.45	0.5	2.87
	$\Psi_N^- \otimes \Lambda_p$	144.2	1.6	0.45	0.5	2.89
^{20}Ne	Ψ_N^+	155.6(160.6)	–	0.38	0.7	2.89
	Ψ_N^-	147.5(155.6)	–	0.43	0.4	2.91
${}^{21}_{\Lambda}$Ne	$\Psi_N^+ \otimes \Lambda_s$	172.8	17.2	0.37	0.7	2.85
	$\Psi_N^+ \otimes \Lambda_p$	162.4	6.75	0.38	0.6	2.88
	$\Psi_N^- \otimes \Lambda_s$	164.5	8.9	0.42	0.4	2.88
	$\Psi_N^- \otimes \Lambda_p$	154.6	7.1	0.43	0.4	2.90

defined as the difference in energy between the ground state of the core nucleus and the hypernuclear states,

$$B_\Lambda = B({}^{A+1}_{\Lambda}X) - B({}^{A}X_{\text{g.s.}}). \tag{21}$$

As a general trend, the shape of the energy curve is not strongly modified by the Λ particle, except for ${}^{13}_{\Lambda}$C, and the

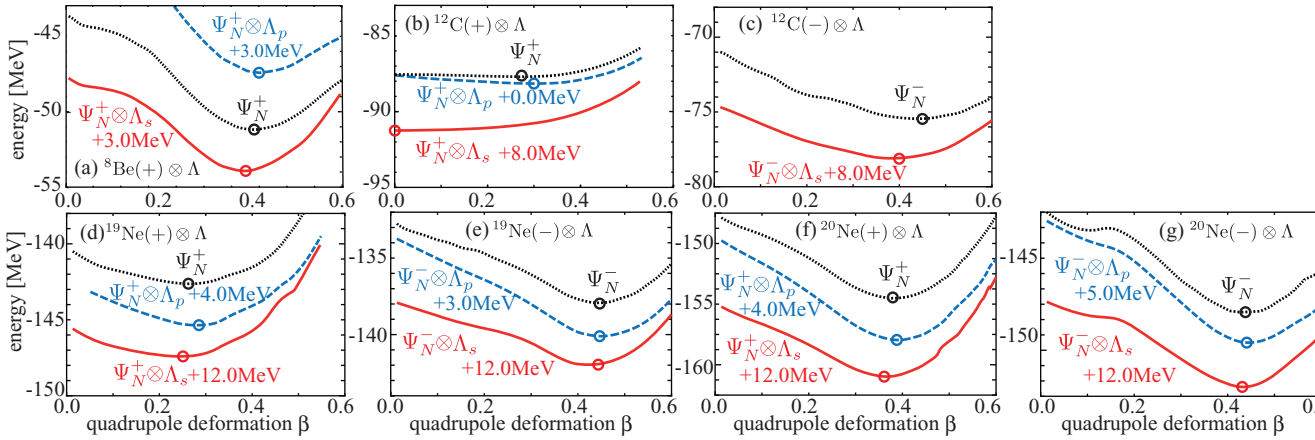

FIG. 1. (Color online) Energy curves as a function of the nuclear quadrupole deformation β for (a) ${}^{9}_{\Lambda}$Be, (b) and (c) ${}^{13}_{\Lambda}$C, (d) and (e) ${}^{20}_{\Lambda}$Ne, and (f) and (g) ${}^{21}_{\Lambda}$Ne. Panels (a), (b), (d), and (f) compare the positive-parity states of normal nuclei (Ψ_N^+) with the hypernuclear states of the $\Psi_N^+ \otimes \Lambda_s$ and $\Psi_N^+ \otimes \Lambda_p$ configurations. Panels (c), (e), and (g) compare the negative-parity states (Ψ_N^-) with the hypernuclear states of the $\Psi_N^- \otimes \Lambda_s$ and $\Psi_N^- \otimes \Lambda_p$ configurations. Open circles show the energy minimum on each curve. Energies of hypernuclei are shifted in the figure for the sake of the presentation.

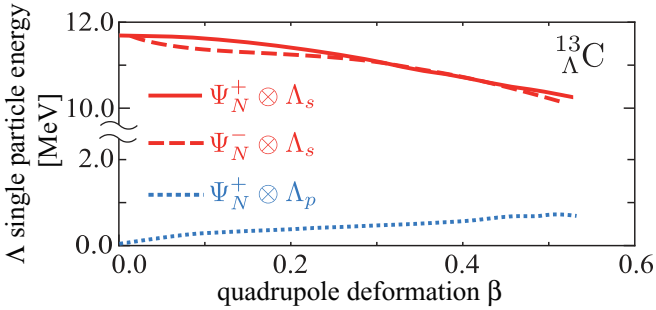

FIG. 2. (Color online) The single-particle energies of Λ_s and Λ_p of $^{13}_{\Lambda}$C as a function of quadrupole deformation of the core nucleus ^{12}C. The solid (dashed) line shows the energy of Λ_s coupled to the positive (negative) parity state of ^{12}C. The dotted line shows the energy of Λ_p coupled to the positive-parity state of ^{12}C.

deformations β at the minima are slightly changed. In all cases, Λ_s reduces quadrupole deformation. This is consistent with cluster model calculations [22,27] and (relativistic) mean-field calculations [3–5] that have demonstrated the reduction of β by Λ_s. On the other hand, it is found that Λ_p increases β. The magnitude of the change in quadrupole deformation is strongly dependent on the core nucleus and is most prominent in $^{13}_{\Lambda}$C, in which Λ_s makes the ^{12}C core spherical, while Λ_p enhances the core deformation. The reasons for the opposite behaviors of Λ_s and Λ_p and the strong dependence on the core nucleus are clearly seen in the single-particle energy of Λ. Figure 2 shows the single-particle energy of Λ [$\epsilon_\Lambda(\beta)$] in each parity and Λ single-particle state in $^{13}_{\Lambda}$C. Here, $\epsilon_\Lambda(\beta)$ is defined as the difference between the binding energy of $^{13}_{\Lambda}$C with deformation β and that of the corresponding state of ^{12}C with the same deformation,

$$\epsilon_\Lambda(\beta) = B_{^{13}_{\Lambda}\mathrm{C}}(\beta) - B_{^{12}\mathrm{C}}(\beta). \quad (22)$$

Figure 2 shows the Nilsson-model-like behavior of the Λ single-particle energy. The binding of Λ_s becomes shallower as deformation becomes larger. In the case of Λ_p, Λ occupies the lowest p wave that comes down as deformation becomes larger. Therefore, Λ_s makes quadrupole deformation smaller, and Λ_p in the lowest p wave makes it larger. The Λ single-particle energy varies within a range less than 2 MeV as a function of quadrupole deformation when that is smaller than the variation of the core nucleus energy. This is also the case for other calculated hypernuclei. This explains why only $^{13}_{\Lambda}$C [Fig. 1(b)] manifests the drastic change in quadrupole deformation. Since the positive-parity state of ^{12}C is quite soft to the quadrupole deformation, a small change in the Λ single-particle energy can result in a large modification in quadrupole deformation. In other cases, a change in the Λ single-particle energy cannot overcome much larger variation of the core energy and results in a minor modification of quadrupole deformation. Therefore, we can conclude that the drastic change of quadrupole deformation by a Λ particle occurs when the core nucleus is quite soft to quadrupole deformation within a range less than 2 MeV. Since the behavior of the energy curve is sensitive to the effective NN interaction [37], the drastic change in $^{13}_{\Lambda}$C may depend on the choice of NN interaction, and this will be investigated in our future work. The behavior of the Λ single-particle energy is also understood from the density distribution of the Λ particle and the core nucleus, as shown in Fig. 3. This figure shows that as nuclear deformation becomes larger, the overlap between the Λ_s and the core wave function becomes smaller (for example, compare the $\Psi^+_N \otimes \Lambda_s$ and $\Psi^-_N \otimes \Lambda_s$ configurations of $^{20}_{\Lambda}$Ne). This leads to the reduction of ΛN attraction. On the contrary, larger deformation makes the overlap larger in the case of Λ_p,

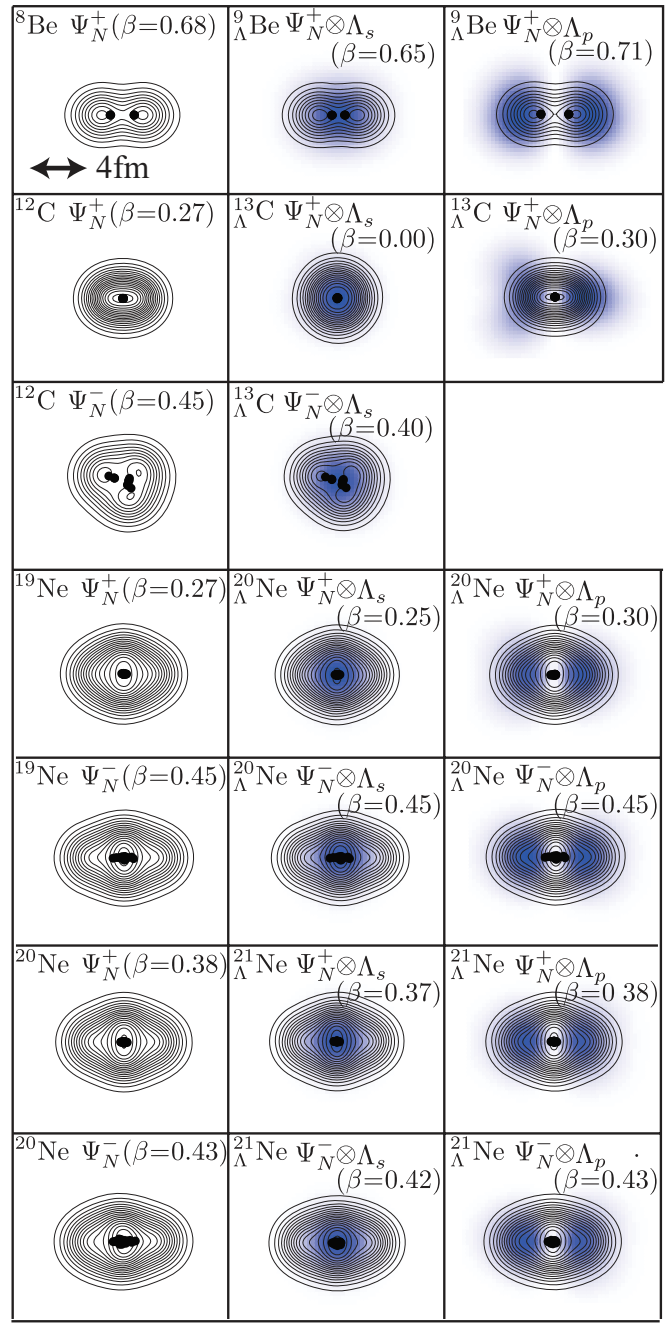

FIG. 3. (Color online) Density plots of the intrinsic wave function at each minimum on the energy curve. Contour lines show the density of the nuclear part Ψ_N, and the color plot shows the Λ single-particle orbital φ_Λ. Dots in the figure show the centroids of Gaussian wave packets on the nuclear part Ψ_N.

and increases ΛN attraction (see $\Psi_N^+ \otimes \Lambda_p$ and $\Psi_N^- \otimes \Lambda_p$ of ${}^{20}_{\Lambda}$Ne). In the case of Λ_p, larger deformation reduces the kinetic energy, which also contributes to the deeper binding of Λ_p.

Another issue to be mentioned is the reduction of the nuclear radius by the Λ particle. In all cases, the radius of the nuclear part is reduced, but the reduction (less than 5%) is much smaller than in the case of ${}^{7}_{\Lambda}$Li (20%) [10]. A more detailed discussion of this point will be found in our next work.

B. Discussion on each hypernucleus

The calculated total binding energies of ^{8}Be and ${}^{9}_{\Lambda}$Be underestimate the observed values by about 5 MeV. The underestimation is common to all other hypernuclei, and can be resolved by performing angular momentum projection and the generator coordinate method (GCM), which are usually performed in the study of normal nuclei by AMD. Indeed, in the case of ^{20}Ne, it was shown that the AMD calculation [15] reproduces the observed binding energy. The angular momentum projection and GCM will also be performed in our next work. Despite the underestimation of the total binding energy, B_Λ of Λ_p is comparable with the observed value.

The density distribution of Λ_p in ${}^{9}_{\Lambda}$Be ($\Psi_N^+ \otimes \Lambda_p$ in Fig. 3) clearly shows that this state corresponds to the supersymmetric (genuine) hypernuclear state [11–13]. The nuclear part has the pronounced 2α cluster structure, and the Λ occupies the p orbital parallel to the symmetry axis. It is also interesting to note that the Λ_s state reduces the intercluster distance, while the Λ_p state increases it.

${}^{13}_{\Lambda}$C manifests a drastic change in quadrupole deformation. The Λ_s makes the ^{12}C core spherical, while the Λ_p state enhances deformation. It is noted that ^{12}C has the $0p_{3/2}$ subshell closure configuration at small deformation, and a 3α cluster structure develops as deformation becomes larger. In other words, the nucleon spin is not saturated at small deformation, while it becomes almost zero at larger deformation. Sophisticated AMD calculation [14] has shown that the low-lying states of ^{12}C have a mixed nature between the $0p_{3/2}$ subshell closure configuration and the 3α cluster structure, and the mixing strength is different for each state. Since the Λ particle changes the deformation and spin properties of ^{12}C, it will have influence on the ΛN spin-orbit splitting of ${}^{13}_{\Lambda}$C [38–40].

Based on the cluster model calculation, the parity inversion in ${}^{20}_{\Lambda}$Ne was suggested by Sakuda and Bandō [7]. The core nucleus ^{19}Ne has the $\alpha + {}^{15}$O cluster state ($J^\pi = 1/2^-_1$) 238 keV above the ground state ($J^\pi = 1/2^+$), which has the $(sd)^3$ shell structure [41]. The researchers conclude that the Λ_s coupled to the $J^\pi = 1/2^-_1$ state was more deeply bound than that coupled to the ground state, and that the $J^\pi = 1/2^- \otimes \Lambda_s$ configuration becomes the ground state of ${}^{20}_{\Lambda}$Ne. They argued that the $J^\pi = 1/2^-_1$ state has a dilute $\alpha + {}^{15}$O cluster structure, and by the reduction of the intercluster distance, Λ_s gains larger binding energy than the $J^\pi = 1/2^+_1 \otimes \Lambda_s$ configuration. Our result shows the opposite trend to their result: Since the positive-parity state is more deformed than the negative-parity state, the binding of Λ_s is weaker when it is coupled to the negative-parity state. This trend is common to other calculations, including the cluster model calculation for ${}^{21}_{\Lambda}$Ne [22]. However, AMD fails to reproduce the small excitation energy of the negative-parity state and does not have prominent $\alpha + {}^{15}$O clustering; both of these results are mainly due to the lack of angular momentum projection and the GCM calculation. We will need a more sophisticated AMD calculation to settle this problem.

The negative-parity state of ^{20}Ne has larger deformation than the positive-parity state. Therefore, the Λ_s coupled to the positive-parity state is more deeply bound than that coupled to the negative-parity state. This is common to the other hypernuclei studied here. On the contrary, Λ_p is more deeply bound to the negative-parity state. Since the number of nucleons in ^{20}Ne is large enough to bound Λ_p, we can expect that the addition of Λ will generate a variety of bound rotational bands in ${}^{21}_{\Lambda}$Ne, as discussed by Yamada *et al.* [22]. We will discuss ${}^{21}_{\Lambda}$Ne in detail in the forthcoming paper.

IV. SUMMARY

An extended version of AMD named HyperAMD has been introduced for investigating the structure of *p-sd* shell hypernuclei. The energy curves of ${}^{9}_{\Lambda}$Be, ${}^{13}_{\Lambda}$C, ${}^{20}_{\Lambda}$Ne, and ${}^{21}_{\Lambda}$Ne as functions of quadrupole deformation were studied, and it was found that Λ_s reduces nuclear deformation, while Λ_p increases it, due to variation of the single-particle energy of Λ as a function of quadrupole deformation. The binding of Λ_s decreases as deformation becomes larger, while that of Λ_p increases. The variation of the Λ single-particle energy is within a range less than 2 MeV, which is rather small compared to the variation of the energy of the core nucleus. Therefore, the magnitude of the change of deformation strongly depends on the softness of the core nucleus to quadrupole deformation. Since ^{12}C is very soft to quadrupole deformation, it manifests the most prominent change of quadrupole deformation. This trend of the deformation change caused by Λ_s and Λ_p contradicts the cluster model calculation for ${}^{20}_{\Lambda}$Ne [7] but is consistent with other calculations. More sophisticated AMD calculations will be needed to resolve this disagreement.

[1] T. Motoba, H. Bandō, and K. Ikeda, Prog. Theor. Phys. **70**, 189 (1983); **71**, 222 (1984).

[2] T. Motoba, H. Bandō, K. Ikeda, and T. Yamada, Prog. Theor. Phys. Suppl. **81**, Chap. 3 (1985).

[3] Xian-Rong Zhou, H.-J. Schulze, H. Sagawa, Chen-Xu Wu, and En-Guang Zhao, Phys. Rev. C **76**, 034312 (2007).

[4] M. T. Win and K. Hagino, Phys. Rev. C **78**, 054311 (2008).

[5] H.-J. Schulze, M. T. Win, K. Hagino, and S. Sagawa, Prog. Theor. Phys. **123**, 569 (2010).

[6] R. H. Dalitz and A. Gal, Phys. Rev. Lett. **36**, 362 (1976).

[7] T. Sakuda and H. Bandō, Prog. Theor. Phys. **78**, 1317 (1987).

[8] U. Straub, Z.-Y. Zhang, K. Bräuer, A. Faessler, and S. B. Khadkikar, Phys. Lett. B **200**, 241 (1988).
[9] T. Yamada, K. Ikeda, H. Bandō, and T. Motoba, Phys. Rev. C **38**, 854 (1988).
[10] K. Tanida *et al.*, Phys. Rev. Lett. **86**, 1982 (2001).
[11] P. H. Pile *et al.*, Phys. Rev. Lett. **66**, 2585 (1991).
[12] O. Hashimoto *et al.*, Nucl. Phys. A **639**, 93c (1998).
[13] O. Hashimoto and H. Tamura, Prog. Part. Nucl. Phys. **57**, 564 (2006), and references therein.
[14] Y. Kanada En'yo, Phys. Rev. Lett. **81**, 5291 (1998).
[15] M. Kimura, Phys. Rev. C **69**, 044319 (2004).
[16] M. Kimura and H. Horiuchi, Nucl. Phys. A **767**, 58 (2006).
[17] W. von Oertzen, Z. Phys. A **354**, 37 (1996).
[18] Y. Kanada En'yo, H. Horiuchi, and A. Ono, Phys. Rev. C **52**, 628 (1995).
[19] N. Itagaki and S. Okabe, Phys. Rev. C **61**, 044306 (2000).
[20] P. Descouvemont, Nucl. Phys. A **699**, 463 (2002).
[21] Y. Kanada En'yo, Phys. Rev. C **66**, 011303 (2002).
[22] T. Yamada, K. Ikeda, H. Bandō, and T. Motoba, Prog. Theor. Phys. **71**, 985 (1984).
[23] A. Reuver, K. Holinde, and J. Speth, Nucl. Phys. A **570**, 543 (1994).
[24] T. A. Rijken and Y. Yamamoto, Phys. Rev. C **73**, 044008 (2006).
[25] Y. Fujiwara, Y. Suzuki, and C. Nakamoto, Prog. Part. Nucl. Phys. **58**, 439 (2007).
[26] D. J. Millener, Nucl. Phys. A **804**, 84 (2008).
[27] E. Hiyama and T. Yamada, Prog. Part. Nucl. Phys. **63**, 339 (2009), and references therein.
[28] A. Dote, H. Horiuchi, and Y. Kanada En'yo, Phys. Rev. C **56**, 1844 (1997).
[29] Y. Sugawa, M. Kimura, and H. Horiuchi, Prog. Theor. Phys. **106**, 1129 (2001).
[30] M. Kimura, Y. Sugawa, and H. Horiuchi, Prog. Theor. Phys. **106**, 1153 (2001).
[31] Y. Kanada En'yo, M. Kimura, and H. Horiuchi, C. R. Phys. **4**, 497 (2003).
[32] Y. Yamamoto, T. Motoba, H. Himeno, K. Ikeda, and S. Nagata, Prog. Theor. Phys. Suppl. **117**, 361 (1994).
[33] H. Matsumiya, M. Kimura, A. Dote, and H. Ohnishi, Phys. Rev. C **83**, 024312 (2011).
[34] J. Dechargé and D. Gogny, Phys. Rev. C **21**, 1568 (1980).
[35] M. Juric *et al.*, Nucl. Phys. B **52**, 1 (1973).
[36] D. H. Davis, Nucl. Phys. A **547**, 369c (1992).
[37] J. A. Maruhn, M. Kimura, S. Schramm, P. G. Reinhard, H. Horiuchi, and A. Tohsaki, Phys. Rev. C **74**, 044311 (2006).
[38] S. Ajimura *et al.*, Phys. Rev. Lett. **86**, 4255 (2001).
[39] E. Hiyama, M. Kamimura, T. Motoba, T. Yamada, and Y. Yamamoto, Phys. Rev. Lett. **85**, 270 (2000).
[40] D. J. Millener, Nucl. Phys. A **691**, 93c (2001).
[41] T. Sakuda and F. Nemoto, Prog. Theor. Phys. **62**, 1274 (1979); **62**, 1606 (1979).